

Activation thresholds in epidemic spreading with motile infectious agents on scale-free networks

Diogo H. Silva¹ and Silvio C. Ferreira^{1,2}

¹⁾Departamento de Física, Universidade Federal de Viçosa, 36570-900 Viçosa, Minas Gerais, Brazil

²⁾National Institute of Science and Technology for Complex Systems, Brazil

We investigate a fermionic susceptible-infected-susceptible model with mobility of infected individuals on uncorrelated scale-free networks with a power-law degree distribution $P(k) \sim k^{-\gamma}$ of exponent $2 < \gamma < 3$. Two diffusive processes with diffusion rate D of an infected vertex are considered. In the *standard diffusion*, one of the nearest-neighbors is chosen with equal chance while in the *biased diffusion* this choice happens with probability proportional to the neighbor's degree. A non-monotonic dependence of the epidemic threshold on D with an optimum diffusion rate D_* , for which the epidemic spreading is more efficient, is found for standard diffusion while monotonic decays are observed in the biased case. The epidemic thresholds go to zero as the network size is increased and the form that this happens depends on the diffusion rule and degree exponent. Analyses on star and max k -core subgraphs explain several features of the diffusive epidemic process. We analytically investigated the dynamics using quenched and heterogeneous mean-field theories. The former present, in general, a better performance for standard and the latter for biased diffusion models, indicating different activation mechanisms of the epidemic phases that are rationalized in terms of hubs or max k -core subgraphs. The transition to the absorbing state is smeared for networks with $\gamma > 2.5$ in the case of biased diffusion while a regular critical transition with diverging fluctuations is found for standard diffusion.

I. INTRODUCTION

Any system that allows an abstract mathematical representation where the vertices are elements connected by edges representing interactions among them can be suited in the complex network framework¹. A network can be characterized by several statistical properties such as the degree distribution probability $P(k)$ that a randomly selected vertex has k contacts (k is called vertex degree). Many real networks as Internet², actor and scientific collaboration³, airport connections^{4,5} possess degree distributions with power-law tails in the form¹ $P(k) \sim k^{-\gamma}$.

The dynamics processes taking place on the top of a network are on an equal footing as its structural properties⁶. The simplest example is a standard random walk, in which a particle lying on the vertices of the network hops to a nearest-neighbor randomly selected. For connected undirected networks, the stationary probability to find a walker on a vertex is proportional to its degree⁷. Since a random walk is a very basic search mechanism, a deeper understanding of this dynamical process can aid the building of efficient strategies to find a specific content in a network⁸. Moreover, the patterns of mobility of individuals is an issue of increasing relevance that nowadays can be experimentally tracked back using bluetooth and Internet⁹, mobile phones¹⁰, or radio-frequency identification devices^{11,12}. Another important class of dynamic processes on networks is the epidemic spreading¹³. It is a remarkable example where an academic problem in complex systems has turned into applications in real processes as the forecast of outbreaks of Ebola¹⁴, H1N5 influenza¹⁵, and Zika virus¹⁶ to mention only a few examples. A kind of epidemic spreading whose importance has increased significantly is the virus dissemination in mobile devices¹⁷.

Relevance of the interplay between diffusion and epidemic spreading in real systems is self-evident since hosts of infectious agents, such as people and mobile devices, are constantly moving being the carriers that promote the quick transition from a localized outbreak to a large scale epidemics^{4,5,15}. Diffusion has been investigated on networks for *bosonic* epidemic processes where the vertices can be simultaneously occupied by several individuals¹⁸ and, in particular, within the context of heterogeneous metapopulations^{19–23} where each vertex consists itself of a subpopulation and the edges represent possibility of interchange of individuals moving from one subpopulation to another according to a mobility rule. When infected and healthy individuals move with the same rate on a metapopulation, the concentration of both types is proportional to the vertex degree²⁰. On lattices, diffusion in bosonic models can lead to complex outcomes such as discontinuous or continuous absorbing-state phase transitions depending on the diffusion rates of infected and susceptible (that can be infected) individuals²⁴.

Epidemic process are commonly investigated within a *fermionic* approach, in which each vertex can host a single individual¹³. Mean-field theories predict equivalent critical properties and evolution for bosonic and fermionic reaction-diffusion processes but they are not identical¹⁸. One fundamental epidemic process with a stationary active state is the susceptible-infected-susceptible (SIS) model¹³ where the vertices can be in one of two states: susceptible, which can be infected, and infected that can transmit the infection. Infected individuals become spontaneously susceptible with rate μ while the susceptible ones in contact with z infected individuals are infected with rate λz . Despite its simplicity, the SIS model on networks with power-law degree distribution presents complex behaviors and has been subject

of intensive research^{13,25}. Some important features of the SIS model have been discussed in its fermionic version as, for example, the value of the epidemic threshold above which the epidemics lasts forever in the thermodynamical limit²⁶, how this limit is approached^{27–30} and the localization of the epidemic activity^{31–36}.

The epidemic threshold of the SIS model on random graphs with power-law degree distribution is null in the thermodynamical limit²⁶, irrespective of the degree exponent γ . The epidemic threshold of the SIS model is commonly investigated using mean-field methods¹³. Two basic ones are the heterogeneous mean-field (HMF)² and quenched mean-field (QMF)³⁷ theories. Recent reviews can be found elsewhere^{13,25}. The former considers a compartmental approach where vertices with the same degree have the same chance to be infected while the latter takes into account the actual structure of network through its adjacency matrix; See section III. The QMF theory is able to capture the asymptotic null threshold analytically expected²⁶ and observed in simulations²⁷ for all values of $\gamma > 2$ while the zero threshold happens only for $2 < \gamma < 3$ in HMF.

In this paper, we investigate a diffusive fermionic SIS model where infected agents hop to their nearest neighbors with rate D . Two rules, with (*biased diffusion*) and without (*standard diffusion*) tendency to higher degree vertices are investigated. We observe that moderate diffusion enhances epidemic activity in hubs and that the threshold^a asymptotically vanishes for both models while the finite-size scaling of the threshold depends strongly on the diffusion model and the degree exponent of the networks. For a fixed size, the standard diffusion model presents an optimum value of D , in which the epidemic threshold is minimal while a monotonic decay is found for biased diffusion. Comparisons between HMF and QMF theories with the thresholds obtained in simulations on scale-free networks with $\gamma < 3$ show, in general, a higher accuracy of QMF for standard and HMF for biased diffusion models indicating different activation mechanisms^{39,40} for these mobility strategies. We also present evidences for a smeared transition³⁶, in which fluctuations of the order parameter (density of infected vertices) are damped in the case of biased diffusion and $\gamma > 2.5$.

The remaining of the paper is organized as follows. In section II we define the diffusive SIS models, briefly review and present the properties of random walks on networks for the investigated mobility rules. The mean-field equations and their stability analyses are presented in section III. The numerical methods are presented in section IV. Simulations are compared with the mean-field theories in Sec. V and the smearing of the transitions

discussed in Sec. VI. The implications and interpretations of the results are presented in section VII. We summarize our conclusions and prospects in section VIII.

II. MODELS

The models consist of the SIS dynamics described in Sec. I with rates λ and μ on a network of N vertices, including diffusion of infected individuals with rate D . The healing rate is fixed as $\mu = 1$ without loss of generality. Diffusion consists of the exchange of states between the infected vertex and one of its nearest-neighbors selected according to a given rule. It worths to stress that the exchange between two infected vertices does not lead to a new state. The absence of diffusion on the susceptible vertices is motivated by simplification of the computer implementation of the stochastic simulations.

We investigated two diffusion rules. In the standard diffusion, the state of an infected vertex i of degree k_i is exchanged with a randomly selected nearest-neighbor j such that the exchange rate from vertex i to j is

$$D_{ij} = \frac{DA_{ij}}{k_i}, \quad (1)$$

where D is the diffusion coefficient and A_{ij} is the adjacency matrix defined as $A_{ij} = 1$ if i and j are connected and $A_{ij} = 0$ otherwise. In the biased diffusion, the exchange is done preferentially with higher degree neighbors. Considering a simple linear relation $D_{ij} \propto A_{ij}k_j$ it can be written as

$$D_{ij} = \frac{DA_{ij}k_j}{k_i\bar{\kappa}_i}, \quad (2)$$

where

$$\bar{\kappa}_i = \frac{1}{k_i} \sum_j A_{ij}k_j \quad (3)$$

is the average degree of the nearest-neighbors of vertex i . This rule can represent, for example, the mobility pattern of persons linked with the place where they live or work⁹. Both models obey the closure condition $\sum_j D_{ij} = D$.

The standard diffusion of a single random walker was solved⁷ and the stationary probability that the walker is on a given vertex is proportional to its degree. Thus, one expects that diffusion will increase the concentration of infected individuals on hubs. In the limit $D \rightarrow \infty$, the infected walker will visit essentially the entire network implying in high mixing where a mean-field regime is expected.

The random walk problem for biased diffusion on uncorrelated network with degree distribution $P(k)$ can be solved using a HMF theory. Let W_k be the probability that the walker is at a vertex of degree k that evolves as

$$\frac{dW_k}{dt} = -DW_k + k \sum_{k'} P(k'|k)D_{k'k}W_{k'}, \quad (4)$$

^a Rigorously, for a finite system the unique asymptotic stationary state is the absorbing one where all vertices are susceptible³⁸. In this work, we deal with an effective finite-size threshold above which the epidemic lifespan becomes extremely large.

where $D_{k'k} = Dk/[k'\bar{\kappa}(k)]$ is the diffusion rate from a vertex of degree k' to a vertex of degree k and $P(k'|k)$ is the probability that a vertex of degree k is connected to a vertex of degree k' . Assuming absence of degree correlations we have⁴¹ $P(k'|k) = k'P(k')/\langle k \rangle$ and $\bar{\kappa}(k) = \langle k^2 \rangle/\langle k \rangle$. In the stationary state, the probability of finding a walker on a vertex of degree k is

$$W_k = \frac{k^2}{\langle k^2 \rangle}, \quad (5)$$

where $\sum_k W_k P(k) = 1$ since the walker must be somewhere on the network. This result indicates a stronger trend to move to the most connected vertices in comparison with the standard diffusion.

III. MEAN-FIELD ANALYSIS

A. HMF theory

Let ρ_k be the density of infected vertices having degree k . Dynamic equations for this quantity is obtained including the diffusive terms in the HMF equations of the original SIS model² and become

$$\begin{aligned} \frac{d\rho_k}{dt} = & -\rho_k + \lambda k(1 - \rho_k) \sum_{k'} P(k'|k) \rho_{k'} \\ & - k\rho_k \sum_{k'} (1 - \rho_{k'}) D_{kk'} P(k'|k) \\ & + k(1 - \rho_k) \sum_{k'} D_{k'k} P(k'|k) \rho_{k'}. \end{aligned} \quad (6)$$

The first and second terms on the right-hand side represent the healing and infection, respectively. The third and fourth terms correspond to the diffusion of infected vertices from or to a vertex of degree k , respectively, reckoning the contribution of vertices with different degrees.

For standard diffusion, we have $D_{kk'} = D/k$. Performing a linear stability analysis of the fixed point $\rho_k = 0$, we obtain the Jacobian matrix $J_{kk'} = -(1 + D)\delta_{kk'} + C_{kk'}$, where

$$C_{kk'} = \left(\lambda + \frac{D}{k'} \right) k P(k'|k). \quad (7)$$

The epidemic threshold is obtained when the largest eigenvalue of the Jacobian Matrix is zero. Assuming that the network is uncorrelated, we have that $C_{kk'}$ has a positive eigenvector $u_k = k$ with associated eigenvalue

$$\Lambda_1 = \lambda \frac{\langle k \rangle}{\langle k^2 \rangle} + D. \quad (8)$$

Since $C_{kk'}$ is irreducible, the Perron-Frobenius theorem⁴² guarantees that it is the largest eigenvalue. Thus, the epidemic threshold is

$$\lambda_c = \frac{\langle k \rangle}{\langle k^2 \rangle}. \quad (9)$$

This expression is exactly the same found for HMF theory of the non-diffusive SIS dynamics² and does not depend on the diffusion coefficient D . The threshold vanishes for $2 < \gamma < 3$ and is finite if $\gamma > 3$ as the network size $N \rightarrow \infty$.

Considering the biased diffusion with $D_{kk'} = Dk'/[k\bar{\kappa}(k)]$ and uncorrelated networks, the Jacobian matrix is

$$J_{kk'} = -(1 + D)\delta_{kk'} + \frac{Dk^2 P(k')}{\langle k^2 \rangle} + \lambda \frac{kk' P(k')}{\langle k \rangle}. \quad (10)$$

We did not find a closed expression for the largest eigenvalue of this Jacobian and analyzed it using numerical diagonalization⁴³.

B. QMF theory

Let ρ_i be the probability that the vertex i is infected. The QMF equation is also obtained introducing the diffusion terms in the non-diffusive equation³² and it becomes

$$\begin{aligned} \frac{d\rho_i}{dt} = & -\rho_i + \lambda(1 - \rho_i) \sum_j A_{ij} \rho_j \\ & - \rho_i \sum_j D_{ij}(1 - \rho_j) + (1 - \rho_i) \sum_j D_{ji} \rho_j. \end{aligned} \quad (11)$$

The meaning of each term is analogous to those of Eq. (6).

Linear stability analysis around $\rho_i = 0$ provides the Jacobian matrix

$$J_{ij} = -(1 + D)\delta_{ij} + \lambda A_{ij} + D_{ji}, \quad (12)$$

where D_{ij} is given by Eqs. (1) and (2) for standard and biased diffusion, respectively. Note that it is a general result regardless of the correlation patterns. The largest eigenvalues of the Jacobians and thus the epidemic thresholds are, in general, obtained with numerical diagonalization⁴³ unless for simple graphs as the one discussed in subsection III C.

C. QMF theory for a leaking star graph

Due to its importance to understand the SIS dynamics on networks^{26,28,29}, we consider a star graph where the center, $i = 0$, is connected to K leaves, $i = 1, 2, \dots, K$. To include the effects of the diffusion outwards the star, we assume that each leaf has degree $k_{\text{leaf}} = \langle k \rangle$ to mimic a hub in a network. These edges change the diffusion rate D_{10} from a leaf to the center ($D_{j0} = D_{10}$ for $j = 2, \dots, K$) and permit that infected individuals in the leaves leak with rate D_{∞} . Diffusion and infection from outside are disregarded. Due to the symmetry we have that $\rho_1 = \rho_2 = \dots = \rho_K$ and the $K + 1$ equations are

reduced to a two-dimensional system

$$\begin{aligned} \frac{d\rho_0}{dt} &= -\rho_0 + \lambda K \rho_1 (1 - \rho_0) - D_{01} K \rho_0 (1 - \rho_1) \\ &\quad + D_{10} K \rho_1 (1 - \rho_0) \end{aligned} \quad (13)$$

$$\begin{aligned} \frac{d\rho_1}{dt} &= -\rho_1 + \lambda \rho_0 (1 - \rho_1) - D_{10} \rho_1 (1 - \rho_0) \\ &\quad + D_{01} \rho_0 (1 - \rho_1) - D_{\emptyset} \rho_1. \end{aligned} \quad (14)$$

A linear stability analysis around $\rho_i = 0$ provides the the Jacobian

$$\mathbb{J} = \begin{bmatrix} -(1 + D_{01}K) & (\lambda + D_{10})K \\ (\lambda + D_{01}) & -(1 + D_{10} + D_{\emptyset}) \end{bmatrix}. \quad (15)$$

For standard diffusion we have $D_{01} = D/K$, $D_{10} = D/\langle k \rangle$ and $D_{\emptyset} = (\langle k \rangle - 1)D/\langle k \rangle$ and setting the largest eigenvalue to be zero we obtain an epidemic threshold

$$\lambda_c = \frac{D(K + \langle k \rangle)}{2K\langle k \rangle} \left[\sqrt{1 + 4K\langle k \rangle \frac{\langle k \rangle(1 + D)^2 - D^2}{D^2(\langle k \rangle + K)^2}} - 1 \right]. \quad (16)$$

Note that for $D \rightarrow 0$ and $K \gg \langle k \rangle$, we recover the known result for QMF theory of non-diffusive SIS on a star graph²⁷ $\lambda_c \simeq 1/\sqrt{K}$. For $K \gg \langle k \rangle$, which represents hubs, and D finite we obtain

$$\lambda_c \simeq \frac{\langle k \rangle(1 + D)^2 - D^2}{DK}. \quad (17)$$

The analysis is very similar for biased diffusion with the only differences that $D_{10} = DK/[K + \langle k \rangle(\langle k \rangle - 1)] \simeq D$ and $D_{\emptyset} = \langle k \rangle(\langle k \rangle - 1)/[K + \langle k \rangle(\langle k \rangle - 1)]$, in which we assume that all vertices outside the star have degree $\langle k \rangle$. The threshold becomes

$$\lambda_c = \frac{D(K + 1)}{2K} \left[\sqrt{1 + 4K \frac{2D + 1}{D^2(K + 1)^2}} - 1 \right]. \quad (18)$$

For $K \gg \langle k \rangle$ and D finite, Eq. (18) yields

$$\lambda_c \simeq \frac{2D + 1}{DK}. \quad (19)$$

Observe that the threshold for standard diffusion presents a minimum at

$$D_* \simeq \sqrt{\frac{\langle k \rangle}{\langle k \rangle - 1}}, \quad (20)$$

while in biased diffusion it varies monotonically with D . These behaviors are confirmed in simulations (see Sec. IV for algorithms and methods) on leaking star graphs shown in Fig. 1.

IV. NUMERICAL METHODS

We investigated the SIS dynamics on leaking star graphs defined in subsection III C and uncorrelated networks of size N with a power-law degree distributions

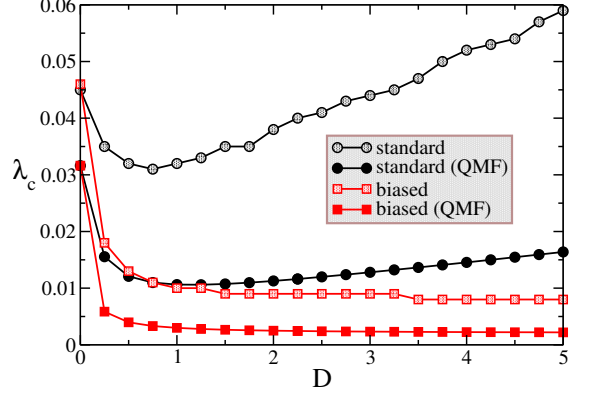


FIG. 1. Epidemic threshold for SIS with standard and biased diffusion on a leaking star graph obtained in QMF theory, Eqs. (16) and (18), and simulations, Sec. IV. A center with $K = 1000$ leaves and each leaf with $\langle k \rangle = 3$ neighbors were used.

$P(k) \sim k^{-\gamma}$. The latter was generated with the uncorrelated configuration model (UCM)⁴⁴ using lower and upper degree cutoffs $k_{\min} = 3$ and $k_{\max} = \sqrt{N}$, respectively, granting absence of the degree correlations in the scale-free regime with $2 < \gamma < 3$.

The algorithm to simulate SIS model with diffusion is based on the optimized Gillespie algorithms with phantom processes⁴⁵ that do not imply in changes of configurations but count for time increments. Let N_{inf} be the number of infected vertices and N_e the sum of the degree of all infected vertices. In each time step, one of the following three events is tried. (i) With probability

$$P_{\text{heal}} = \frac{\mu N_{\text{inf}}}{(\mu + D)N_{\text{inf}} + \lambda N_e}, \quad (21)$$

a randomly selected vertex is spontaneously healed. (ii) With probability

$$P_{\text{inf}} = \frac{\lambda N_e}{(\mu + D)N_{\text{inf}} + \lambda N_e}, \quad (22)$$

one infected vertex is chosen with probability proportional to its degree and one of its nearest-neighbors is selected with equal chance. If the neighbor is susceptible it becomes infected. (iii) Finally, with probability

$$P_{\text{dif}} = \frac{DN_{\text{inf}}}{(\mu + D)N_{\text{inf}} + \lambda N_e}, \quad (23)$$

the states of an infected vertex and one of its nearest-neighbors are exchanged. The target neighbor is chosen with equal chance in standard diffusion and with a probability proportional to its degree in biased diffusion. The time is incremented by $dt = -\ln(u)/[(\mu + d)N_{\text{inf}} + \lambda N_e]$, where u is a pseudo random number uniformly distributed in the interval $(0, 1)$, while N_{inf} and N_e are updated accordingly.

We apply the standard quasistationary method⁴⁶, in which the dynamics is reactivated to some previously

visited configuration, to deal with the absorbing state with $N_{\text{inf}} = 0$ in a finite size system near to the transition point. Implementation details can be found elsewhere^{45,47}. The quasistationary probability \bar{P}_n that the system has n infected vertices near the transition is computed over a time interval $t_{\text{av}} = 10^7$ after a relaxation time $t_{\text{rel}} = 10^6$. Larger or smaller values were used for very subcritical and supercritical simulations, respectively. We analyze the quasistationary density $\langle \rho \rangle$, which is the order parameter that defines active and inactive phases, and the dynamical susceptibility²⁷

$$\chi = N \frac{\langle \rho^2 \rangle - \langle \rho \rangle^2}{\langle \rho \rangle}. \quad (24)$$

whose the position of the maximum yields the effective (size-dependent) epidemic threshold.

V. THEORY VS SIMULATIONS

In this section we compare the thresholds obtained in the mean-field theories with quasistationary simulations.

A. Leaking star graphs

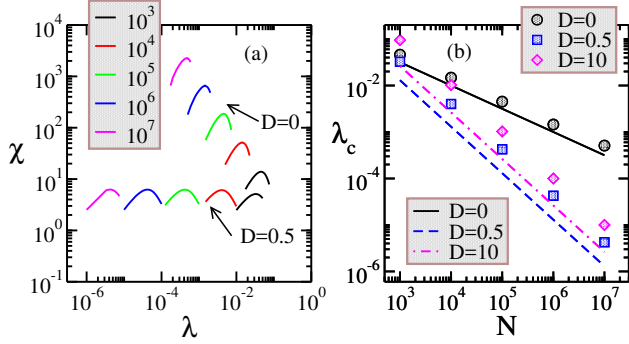


FIG. 2. (a) Susceptibility as a function of the infection rate for leaking star graphs of different sizes (shown in the legends) with $\langle k \rangle = 3$. The cases without diffusion ($D = 0$) and with small standard diffusion rate ($D = 0.5$) are shown. (b) Threshold as a function of the network size for different values of D obtained with simulations (symbols) and QMF theory (lines).

The QMF predictions given by Eq. (18) are compared with simulations on leaking star graphs in Figs. 1 and 2. We see that the theory correctly predicts the qualitative dependence on D for a fixed size, Fig. 1, as well as the scaling of the threshold as a function of the size, Fig. 2(b), regardless of $D > 0$. The susceptibility diverges as the network size increases in agreement with a critical transition⁴⁸ in absence of diffusion^{27,49} while it saturates in the presence of diffusion indicating the smearing of the phase transition where fluctuations do not increase algebraically with the network size⁵⁰. The discussion of smearing is resumed in section VI.

B. Power-law networks with $2 < \gamma < 2.5$

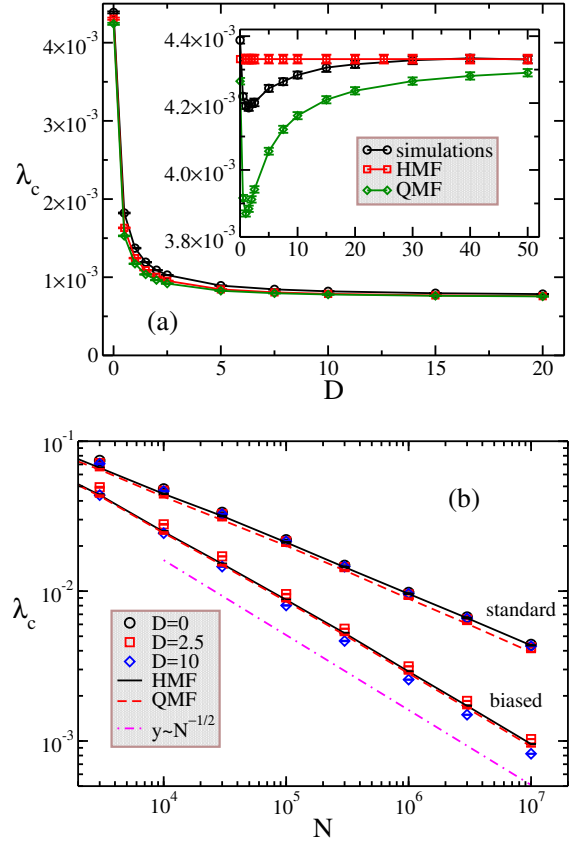


FIG. 3. Epidemic thresholds for the diffusive SIS models on UCM networks with degree exponent $\gamma = 2.25$. (a) Dependence with diffusion rate for a network of size $N = 10^7$. Main panel shows biased while inset standard diffusion models. (b) Finite-size analysis of the epidemic threshold for both diffusion models. The scaling predicted for a star subgraph with $K = k_{\text{max}} \simeq \sqrt{N}$, $\lambda_c^{(\text{star})} \sim N^{-1/2}$, is also shown.

We compare the epidemic thresholds of simulations for UCM networks with $\gamma = 2.25$ with mean-field theories for both diffusion models in Fig. 3. The curves show a dependence with the diffusion coefficient D qualitatively described by QMF but quantitatively better fitted by the HMF theory. Observe the narrow scale for the threshold variation in the standard diffusion in the inset of Fig. 3(a). We observe a quantitative good agreement between simulations and HMF and QMF theories in both models, which is evident in the finite-size analysis shown in Fig. 3(b). The standard diffusion presents scaling with size in agreement with the HMF theory given by $\lambda_c^{(\text{HMF})} = \langle k \rangle / \langle k^2 \rangle \sim k_{\text{max}}^{\gamma-3} \sim N^{-0.375}$ for $\gamma = 2.25$. The scaling for biased diffusion is also captured by the HMF theory but it additionally coincides with that of a leaking star subgraph centered on the most connected vertex that scales as $\lambda_c^{(\text{star})} \sim k_{\text{max}}^{-1} \sim N^{-1/2}$.

C. Power-law networks with $2.5 < \gamma < 3$

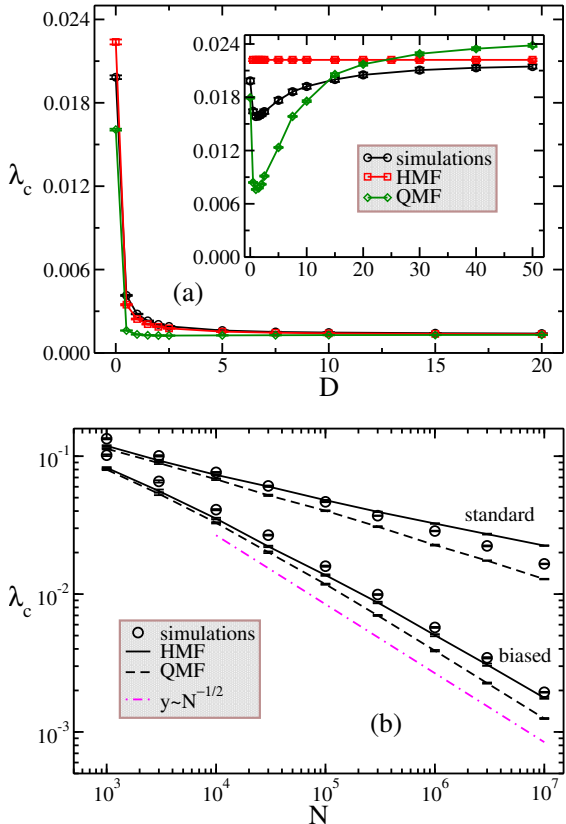


FIG. 4. Epidemic thresholds for the diffusive SIS model on UCM networks with degree exponent $\gamma = 2.75$. (a) Dependence with the diffusion rate for a network of size $N = 10^7$. The main panel shows biased while the inset standard diffusion models. (b) Finite-size analysis of the epidemic threshold for both diffusion models with $D = 2.5$. The scaling predicted for the epidemic threshold on a leaking star graph with $K = k_{\max} \simeq \sqrt{N}$, $\lambda_c^{(\text{star})} \sim N^{-1/2}$, is also shown.

The curves $\lambda_c(D)$ for UCM networks with fixed size $N = 10^7$ and exponent $\gamma = 2.75$ are shown in Fig. 4(a). The qualitative picture observed for $\gamma < 2.5$ does not change with the presence of an optimum value where the threshold is minimum in the case of standard diffusion. Quantitatively, a considerably larger variability of the threshold as a function of D is found for standard diffusion. Another difference for large D is that QMF deviates from both HMF theory and simulations. The last two converge to each other. Theory performances for standard and biased diffusions can be seen in the finite-size analysis of the threshold for a fixed diffusion coefficient in Fig. 4(b). While standard diffusion is quantitatively better fitted by the QMF than HMF theory, as in the non-diffusive case^{27,49}, the biased diffusion is clearly better described by the HMF theory, which predicts accurately both scaling and amplitude of the epidemic threshold as a function of size. Within the investigated size range, the threshold decay in QMF theory for the biased diffi-

fusion asymptotically scale as that of a leaking star subgraph centered on the most connected vertex with degree $K \simeq \sqrt{N}$, $\lambda_c \sim N^{-1/2}$, but this was not observed for standard diffusion.

VI. SMEARING OF THE TRANSITION

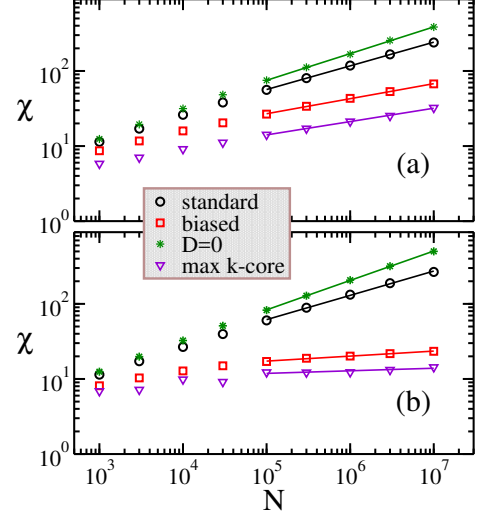


FIG. 5. Finite-size analyses of the susceptibility maxima. Two diffusive SIS models with $D = 2.5$ for (a) $\gamma = 2.25$ and (b) $\gamma = 2.75$ are shown. The susceptibilities without diffusion and for a subgraph containing only the max k -core are shown for sake of comparison. Lines are power-law regressions.

A smeared phase transition occurs when a system undergoes a change of phase without diverging fluctuations of the order parameter⁵⁰. This happens, for example, in the presence of sub-extensive metastable regions that eventually become inactive by some rare fluctuation⁵⁰. This type of transition has been reported for the non-diffusive SIS model on UCM networks with $\gamma > 3$ and the associated sub-extensive active patches are the hubs plus their nearest-neighbors^{36,40}. In the context of a smeared transition on networks, the dynamical susceptibility at the transition remains bounded in the thermodynamical limit. Both diffusive dynamics in leaking star graphs clearly present smeared transitions, as be can seen in Fig. 2(a) for standard diffusion.

The susceptibility at the transition point was fitted to a simple power-law in the form

$$\chi(\lambda_c) \sim N^\phi \quad (25)$$

for sizes $N \geq 10^5$. The exponents obtained for the non-diffusive SIS were $\phi \approx 0.35$ for $\gamma = 2.25$ and $\phi \approx 0.39$ for $\gamma = 2.75$ which are in agreement with values reported elsewhere⁴⁰. Standard diffusion does not produce visible smearing of the transition for both investigated values of $\gamma = 2.25$ and $\gamma = 2.75$ as can seen in Fig. 5 and in the scaling exponents shown in Table I. Different scenarios

for $\gamma = 2.25$ and 2.75 are obtained for biased diffusion. For $\gamma = 2.25$, the exponent $\phi \approx 0.20$ is the same, within uncertainties, for both values of D that we investigated. For $\gamma = 2.75$, the regression provides a small exponent that may indicate a saturation consistent with a smearing of the phase transition.

TABLE I. Exponents of the finite-size scaling of the maximal susceptibility values defined as $\chi(\lambda_c) \sim N^\phi$. The simulations were run on networks with power-law degree distributions. Uncertainties shown in parenthesis were determined using different fitting regions and aims at showing the distinction or similarities among exponents rather than the accuracy in their estimates.

Model	$\gamma = 2.25$		$\gamma = 2.75$	
	$D = 2.5$	$D = 10$	$D = 2.5$	$D = 10$
standard	0.315(5)	0.281(3)	0.320(6)	0.323(6)
biased	0.200(5)	0.201(2)	0.063(5)	0.071(2)

VII. DISCUSSION

We start our discussion with the epidemic threshold dependence on the diffusion coefficient D for a fixed network size. The non-monotonic dependence on D for the standard and the monotonic decay for biased diffusion models regardless of the degree exponent γ seem to be reminiscent of the hub activation since they qualitatively agree with the threshold obtained for leaking star graph shown in Fig. 1 and are qualitatively captured by the QMF theory. The role played by diffusion in the activation of hubs is stronger in the biased case, as initially suggested by the analysis of random walks in Sec. II, in which a much higher tendency to move towards hubs is found with biased diffusion. Despite the different thresholds, both dynamics are well described by HMF theory in the high diffusion limit, which is expected since high mobility promotes mixing and breaks down pairwise dynamical correlations. In such a regime HMF theory becomes exact in the thermodynamical limit.

The finite-size scaling of the epidemic threshold in a size range $10^3 < N < 10^7$ shows further differences with respect to the performance of the mean-field theories. For $\gamma < 2.5$, both QMF and HMF theories have good performance for both models. However, for $2.5 < \gamma < 3$ the standard diffusion is better described by QMF while HMF presents a much better performance for biased diffusion.

Two different mechanisms have been associated to the activation of the epidemics in the non-diffusive SIS model on uncorrelated scale-free networks³⁹. A discussion for a more general epidemics can be found elsewhere⁵¹. For $\gamma < 2.5$, the epidemics in SIS is triggered in a densely connected component of the network identified by the

maximum index of a k -core decomposition^b, hereafter called of max k -core. For $\gamma > 2.5$ this activation is triggered in the largest hubs of the network. The max k -core activation mechanism was described by a HMF theory, which is an intrinsically collective theory due to its close relation with annealed networks⁵³, while the hub mechanism is better suited within a QMF theory involving a few elements of the network, namely the hubs. This conjecture relating activation mechanisms and suitability of mean-field theories has been verified for other epidemic models^{40,54}. Following this conjecture, we have that the activation happens in the max k -core for the biased diffusion in the whole range $2 < \gamma < 3$ and follows the same scheme of the non-diffusive SIS for the standard diffusion, with hub triggering activation for $\gamma > 2.5$.

TABLE II. Exponents of the finite size scaling of the maximal susceptibility values defined as $\chi(\lambda_c) \sim N^\phi$. The simulations were run on the max k -core of networks with power-law degree distributions. See table I for uncertainties meaning.

Model	$\gamma = 2.25$		$\gamma = 2.75$	
	$D = 2.5$	$D = 10$	$D = 2.5$	$D = 10$
standard	0.178(2)	0.178(1)	0.06(3)	0.07(2)
biased	0.176(2)	0.179(1)	0.03(1)	0.04(2)

The smearing observed in star graphs happens because the center is reinfected almost instantaneously after it becomes susceptible since the total diffusion rate to the center is proportional to $N_{\text{inf}}D \gg 1$, where N_{inf} is the number of infected leaves. The center constantly infected depletes fluctuations in the number of infected individuals which controls the order parameter. The smeared phase transition suggested for the biased diffusion for $\gamma = 2.75$ but not for $\gamma = 2.25$ in principle could suggest that the activation mechanisms for these two degree exponents are different. However, the susceptibility computed in simulations restricted to the max k -core are consistent with smearing for $\gamma = 2.75$ but not for $\gamma = 2.25$ as can be seen in Fig. 5 and in the exponents given in table II. Notice that the scaling exponents are the same within uncertainties for both diffusion models that also agree with the exponent of the non-diffusive case, in contrast with the clearly distinct exponents in the simulations over the whole networks shown in table I.

We could naturally wonder why do biased and standard diffusion models behave so differently if mobility

^b A k -core decomposition⁵² consists of a pruning process that starts removing all vertices with degree $k_s = k_{\min}$ plus their edges and any other vertex whose degree became k_{\min} after the removal, until no more vertices of degree k_{\min} are present. The procedure is sequentially repeated for $k_s = k_{\min} + 1$, $k_{\min} + 2$ and so on until all vertices are removed. The max k -core corresponds to the subset of vertices and edges removed in the last step of the decomposition.

favors localization in hubs for both cases? A high diffusivity implies that the infected individual stays shortly in a same vertex. In standard diffusion, when the infected individual leaves a hub towards a randomly selected neighbor, it more probably arrives at a low degree vertex, present in a much larger number, where it spreads the infection less efficiently. So, even enhancing mobility to higher degree vertices, the net effect of sufficiently high standard diffusion is to reduce the infection power of hubs. In the biased diffusion, the mobility towards hubs is highly favored such that the infected individual stays moving mostly among hubs keeping, therefore, its spreading efficiency at high levels. Moreover, these high degree vertices belong to the max k -core in random scale-free networks in consonance with the activation mechanism for $2.5 < \gamma < 3$ in the biased diffusion model.

VIII. CONCLUDING REMARKS

Mobility is a fundamental promoter of epidemic spreading in real world and its effects on epidemic models on networks have been dealt in the context of bosonic processes where a single vertex can host several infected individuals²⁰. A lot of theoretical attention has been dedicated to the investigation of fermionic epidemic models where no more than one individual can lay in a vertex¹³. However, the effects of mobility in the fermionic epidemic models on networks have been not addressed thoroughly. We consider the role played by mobility in the phase transition of two fermionic diffusive SIS models on scale-free networks with degree distribution $P(k) \sim k^{-\gamma}$ and exponent $2 < \gamma < 3$. Both standard and biased diffusion models were considered. In the latter, higher degree vertices are favored.

The epidemic thresholds were investigated on large networks using stochastic simulations and compared with QMF and HMF theories. Biases reduce significantly the epidemic threshold for a fixed network size, and is very well described by the HMF theory. Standard diffusion yields a non-monotonic dependence on D with an optimum value D_* where the threshold at a given size is minimum. QMF theory describes better the epidemic threshold for standard diffusion. Different triggering mechanisms of the epidemic phase were identified. While biased diffusion leads to a max k -core activation for all values of $2 < \gamma < 3$, the standard diffusion behaves as the non-diffusive case, being activated by hubs for $\gamma > 2.5$ and max k -core for $\gamma < 2.5$. We also report a smearing of the phase transition for the biased model with exponent $2.5 < \gamma < 3$.

Our study reveals non-trivial effects of the mobility on the outcomes of epidemic models running on the top of heterogeneous networks. We expect that it will render impacts for forthcoming research in the field. Theoretically, the case $\gamma > 3$ needs further attention. Our first analysis points out a very strong smearing which depletes the fluctuations, markedly changing the nature of the

epidemic transition. From the application point of view, the role of correlation and assortativity patterns, which are ubiquitous in real networked systems, as well as the mobility of susceptible individuals call for additional investigations.

ACKNOWLEDGMENTS

This work was partially supported by the Brazilian agencies CAPES, CNPq and FAPEMIG. S.C.F. thanks the support from the program *Ciência sem Fronteiras* - CAPES under project No. 88881.030375/2013-01.

- ¹A.-L. Barabási and M. Pósfai, *Network science* (Cambridge University Press, Cambridge, UK, 2016).
- ²R. Pastor-Satorras, A. Vázquez, and A. Vespignani, “Dynamical and correlation properties of the internet,” *Phys. Rev. Lett.* **87**, 258701 (2001).
- ³J. J. Ramasco, S. N. Dorogovtsev, and R. Pastor-Satorras, “Self-organization of collaboration networks,” *Phys. Rev. E* **70**, 036106 (2004).
- ⁴V. Colizza, A. Barrat, M. Barthelemy, and A. Vespignani, “The role of the airline transportation network in the prediction and predictability of global epidemics,” *Proc. Natl. Acad. Sci.* **103**, 2015–2020 (2006).
- ⁵A. Vespignani, “Modelling dynamical processes in complex socio-technical systems,” *Nat. Phys.* **8**, 32–39 (2012).
- ⁶A. Barrat, M. Barthelemy, and A. Vespignani, *Dynamical Processes on Complex Networks* (Cambridge University Press, Cambridge, UK, 2008).
- ⁷J. D. Noh and H. Rieger, “Random walks on complex networks,” *Phys. Rev. Lett.* **92**, 118701 (2004).
- ⁸N. Masuda, M. A. Porter, and R. Lambiotte, “Random walks and diffusion on networks,” *Phys. Rep.* **716-717**, 1–58 (2017).
- ⁹N. Eagle and A. Pentland, “Reality mining: sensing complex social systems,” *Pers. Ubiquitous Comput.* **10**, 255–268 (2006).
- ¹⁰M. C. González, C. A. Hidalgo, and A.-L. Barabási, “Understanding individual human mobility patterns,” *Nature* **453**, 779–782 (2008).
- ¹¹C. Cattuto, W. Van den Broeck, A. Barrat, V. Colizza, J.-F. Pinton, and A. Vespignani, “Dynamics of person-to-person interactions from distributed RFID sensor networks,” *PLoS One* **5**, e11596 (2010).
- ¹²J. Stehlé, N. Voirin, A. Barrat, C. Cattuto, L. Isella, J.-F. Pinton, M. Quaggiotto, W. Van den Broeck, C. Régis, B. Lina, and P. Vanhems, “High-resolution measurements of face-to-face contact patterns in a primary school,” *PLoS One* **6** (2011).
- ¹³R. Pastor-Satorras, C. Castellano, P. Van Mieghem, and A. Vespignani, “Epidemic processes in complex networks,” *Rev. Mod. Phys.* **87**, 925–979 (2015).
- ¹⁴M. F. C. Gomes, A. Pastore y Piotti, L. Rossi, D. Chao, I. Longini, and M. E. Halloran, “Assessing the international spreading risk associated with the 2014 west african ebola outbreak,” *PLoS Curr.* **19**, 1–22 (2014).
- ¹⁵V. Colizza, A. Barrat, M. Barthelemy, A.-J. Valleron, and A. Vespignani, “Modeling the worldwide spread of pandemic influenza: Baseline case and containment interventions,” *PLoS Med.* **4**, e13 (2007).
- ¹⁶Q. Zhang, K. Sun, M. Chinazzi, A. Pastore y Piontti, N. E. Dean, D. P. Rojas, S. Merler, D. Mistry, P. Poletti, L. Rossi, M. Bray, M. E. Halloran, I. M. Longini, and A. Vespignani, “Spread of Zika virus in the Americas,” *Proc. Natl. Acad. Sci.* **114**, E4334–E4343 (2017).
- ¹⁷P. Wang, M. C. Gonzalez, C. A. Hidalgo, and A.-L. Barabási, “Understanding the spreading patterns of mobile phone viruses,” *Science* **324**, 1071–1076 (2009).

¹⁸A. Baronchelli, M. Catanzaro, and R. Pastor-Satorras, “Bosonic reaction-diffusion processes on scale-free networks,” *Phys. Rev. E* **78**, 016111 (2008).

¹⁹M. J. Keeling and C. A. Gilligan, “Metapopulation dynamics of bubonic plague,” *Nature* **407** (2000).

²⁰V. Colizza, R. Pastor-Satorras, and A. Vespignani, “Reaction-diffusion processes and metapopulation models in heterogeneous networks,” *Nat. Phys.* **3**, 276–282 (2007).

²¹V. Colizza and A. Vespignani, “Invasion threshold in heterogeneous metapopulation networks,” *Phys. Rev. Lett.* **99**, 148701 (2007).

²²A. S. Mata, S. C. Ferreira, and R. Pastor-Satorras, “Effects of local population structure in a reaction-diffusion model of a contact process on metapopulation networks,” *Phys. Rev. E* **88**, 042820 (2013).

²³J. Gómez-Gardeñes, D. Soriano-Paños, and A. Arenas, “Critical regimes driven by recurrent mobility patterns of reaction-diffusion processes in networks,” *Nat. Phys.* **14**, 391–395 (2018).

²⁴D. S. Maia and R. Dickman, “Diffusive epidemic process: theory and simulation,” *J. Phys. Condens. Matter* **19**, 065143 (2007).

²⁵W. Wang, M. Tang, H. Eugene Stanley, and L. A. Braunstein, “Unification of theoretical approaches for epidemic spreading on complex networks,” *Reports Prog. Phys.* **80**, 036603 (2017).

²⁶S. Chatterjee and R. Durrett, “Contact processes on random graphs with power law degree distributions have critical value 0,” *Ann. Probab.* **37**, 2332–2356 (2009).

²⁷S. C. Ferreira, C. Castellano, and R. Pastor-Satorras, “Epidemic thresholds of the susceptible-infected-susceptible model on networks: A comparison of numerical and theoretical results,” *Phys. Rev. E* **86**, 041125 (2012).

²⁸C. Castellano and R. Pastor-Satorras, “Thresholds for epidemic spreading in networks,” *Phys. Rev. Lett.* **105**, 218701 (2010).

²⁹M. Boguñá, C. Castellano, and R. Pastor-Satorras, “Nature of the epidemic threshold for the susceptible-infected-susceptible dynamics in networks,” *Phys. Rev. Lett.* **111**, 068701 (2013).

³⁰C.-R. Cai, Z.-X. Wu, M. Z. Q. Chen, P. Holme, and J.-Y. Guan, “Solving the dynamic correlation problem of the susceptible-infected-susceptible model on networks,” *Phys. Rev. Lett.* **116**, 258301 (2016).

³¹A. S. Mata and S. C. Ferreira, “Multiple transitions of the susceptible-infected-susceptible epidemic model on complex networks,” *Phys. Rev. E* **91**, 012816 (2015).

³²A. V. Goltsev, S. N. Dorogovtsev, J. G. Oliveira, and J. F. F. Mendes, “Localization and spreading of diseases in complex networks,” *Phys. Rev. Lett.* **109**, 128702 (2012).

³³H. K. Lee, P.-S. Shim, and J. D. Noh, “Epidemic threshold of the susceptible-infected-susceptible model on complex networks,” *Phys. Rev. E* **87**, 062812 (2013).

³⁴G. St-Onge, J.-G. Young, E. Laurence, C. Murphy, and L. J. Dubé, “Phase transition of the susceptible-infected-susceptible dynamics on time-varying configuration model networks,” *Phys. Rev. E* **97**, 022305 (2018).

³⁵G. Ódor, “Spectral analysis and slow spreading dynamics on complex networks,” *Phys. Rev. E* **88**, 32109 (2013).

³⁶W. Cota, S. C. Ferreira, and G. Ódor, “Griffiths effects of the susceptible-infected-susceptible epidemic model on random power-law networks,” *Phys. Rev. E* **93**, 032322 (2016).

³⁷D. Chakrabarti, Y. Wang, C. Wang, J. Leskovec, and C. Faloutsos, “Epidemic thresholds in real networks,” *ACM Trans. Inf. Syst. Secur.* **10**, 1:1–1:26 (2008).

³⁸J. Marro and R. Dickman, *Nonequilibrium Phase Transitions in Lattice Models* (Cambridge University Press, Cambridge UK, 2005).

³⁹C. Castellano and R. Pastor-Satorras, “Competing activation mechanisms in epidemics on networks,” *Sci. Rep.* **2**, 371 (2012).

⁴⁰W. Cota, A. S. Mata, and S. C. Ferreira, “Robustness and fragility of the susceptible-infected-susceptible epidemic models on complex networks,” *Phys. Rev. E* **98**, 012310 (2018).

⁴¹M. Boguñá and R. Pastor-Satorras, “Class of correlated random networks with hidden variables,” *Phys. Rev. E* **68**, 036112 (2003).

⁴²M. Newman, *Networks: An Introduction* (OUP Oxford, 2010).

⁴³W. H. Press, *Numerical Recipes* (Cambridge University Press, Cambridge, UK, 2007).

⁴⁴M. Catanzaro, M. Boguñá, and R. Pastor-Satorras, “Generation of uncorrelated random scale-free networks,” *Phys. Rev. E* **71**, 027103 (2005).

⁴⁵W. Cota and S. C. Ferreira, “Optimized gillespie algorithms for the simulation of markovian epidemic processes on large and heterogeneous networks,” *Comput. Phys. Commun.* **219**, 303–312 (2017).

⁴⁶M. M. de Oliveira and R. Dickman, “How to simulate the quasistationary state,” *Phys. Rev. E* **71**, 016129 (2005).

⁴⁷R. S. Sander, G. S. Costa, and S. C. Ferreira, “Sampling methods for the quasistationary regime of epidemic processes on regular and complex networks,” *Phys. Rev. E* **94**, 042308 (2016).

⁴⁸U. C. Tauber, *Critical Dynamics* (Cambridge University Press, Cambridge, UK, 2014).

⁴⁹A. S. Mata and S. C. Ferreira, “Pair quenched mean-field theory for the susceptible-infected-susceptible model on complex networks,” *EPL (Europhysics Lett.)* **103**, 48003 (2013).

⁵⁰T. Vojta, “Rare region effects at classical, quantum and nonequilibrium phase transitions,” *J. Phys. A. Math. Gen.* **39**, R143–R205 (2006).

⁵¹M. Kitsak, L. K. Gallos, S. Havlin, F. Liljeros, L. Muchnik, H. E. Stanley, and H. A. Makse, “Identification of influential spreaders in complex networks,” *Nat. Phys.* **6**, 888–893 (2010).

⁵²S. N. Dorogovtsev, A. V. Goltsev, and J. F. F. Mendes, “ k -core organization of complex networks,” *Phys. Rev. Lett.* **96**, 040601 (2006).

⁵³M. Boguñá, C. Castellano, and R. Pastor-Satorras, “Langevin approach for the dynamics of the contact process on annealed scale-free networks,” *Phys. Rev. E* **79**, 036110 (2009).

⁵⁴S. C. S. Ferreira, R. R. S. Sander, and R. Pastor-Satorras, “Collective versus hub activation of epidemic phases on networks,” *Phys. Rev. E* **93**, 032314 (2016).